International Conference "Water, Environment, Energy and Society" (WEES–2009)
New Delhi, 12–16 January 2009

Forecasting Spatiotemporal Water Levels of Tabriz Aquifer

V. Nourani
Faculty of Civil Engineering
Tabriz University, IRAN
E-mail: nourani@tabrizu.ac.ir

A.A. Moghaddam[1] and A.O. Nadiri
Department of Geology
Faculty of Science, Tabriz University, IRAN
E-mail: [1]moghaddam@tabrizu.ac.ir

V.P. Singh
Department of Biological and Agricultural Engineering
Texas A&M University, USA
E-mail: vsingh@tamu.edu

ABSTRACT: This paper evaluates the feasibility of using an Artificial Neural Networks (ANNs) methodology for estimating the groundwater level in some piezometers placed in an aquifer in northwestern Iran. This aquifer is complex and has a high water level in urban areas. Spatiotemporal groundwater level simulation in a multilayer aquifer is regarded as a difficult subject in hydrogeology due to complexity and different aquifer materials. In the present research the performance of different neural networks for groundwater level forecasting is examined, in order to identify an optimal ANN architecture that can simulate selected piezometer water levels and provide acceptable predictions up to 24 months ahead. Six different types of network architectures and training algorithms are investigated and compared in terms of model prediction efficiency and accuracy. The results of different experiments show that accurate predictions can be achieved with a standard feedforward neural network trained with the Levenberg–Marquardt algorithm. Obtained structure and spatial regression relations of the ANN parameters (weights and biases) are used for spatiotemporal model presentation. It was found in this study that ANNs provided accurate predictions when an optimum number of spatial and temporal inputs were included into the network, and that the network with lower lag consistently produced better performance.

Keywords: Artificial Neural Networks (ANNs) Model, Groundwater Level, Spatiotemporal Forecasting, Tabriz Aquifer.

INTRODUCTION

Although conceptual and physically-based models are the main tool for depicting hydrological variables and understanding the physical processes taking place in a system, they do have practical limitations. When data is not sufficient and getting accurate predictions is more important than conceiving the actual physics, empirical models remain a good alternative, and can provide useful results without costly calibration. ANN models are such 'black box' models with particular properties which are greatly suited to dynamic nonlinear system modeling. The advantages of ANN models over conventional simulation methods have been discussed in detail by French *et al.* (1992). ANN applications in hydrology vary from real-time to event based modeling. ANN models have been used for rainfall-runoff modeling, precipitation forecasting and water quality modeling (Govindaraju and Ramachandra Rao, 2000). One of the most important features of ANN models is their ability to adapt to recurrent changes and detect patterns in a complex natural system. More concepts and applications of ANN models in hydrology have been discussed by the ASCE (2000). Neural networks have also been previously applied with success to groundwater level prediction (Coulibaly *et al.*, 2001a, b, c). The ANN methodology has also been applied to forecast rainfall (Luck Kin *et al.*, 2001). Parkin *et al.* (2001) used ANNs, coupled with a 3-D numerical model, to model river-aquifer interactions. In the geotechnical domain, Kurup and Dudani (2002) used ANN to profile the stress history of clays from piezocone penetration tests. In chalky media, some researches can be mentioned, for example, as regards forecasting of

turbid floods in a karstic media (Beaudeau *et al.*, 2001) and determination of aquifer outflow influential parameters, and simulation and forecasting of aquifer outflow in a fissured chalky media (Lallahem and Mania, 2002, 2003a, b). Recently, ANNs have been successfully used for identifying the temporal data necessary to calculate groundwater level in only one piezometer (Lallahem *et al.*, 2005). In this paper, several different neural networks are evaluated in order to reach conclusions regarding the efficiency of forecasting techniques for groundwater level prediction and finding a good technique for presenting spatiotemporal ANN model for Tabriz aquifer.

THE ARTIFICIAL NEURAL NETWORKS APPROACH

The Basics

An ANN is a computational approach inspired by the human nervous system. Its data processing paradigm is made up of highly interconnected nodes (neurons) that map a complex input pattern with a corresponding output pattern (Kohonen, 1988; Hagan *et al.*, 1996). ANN is used to define the network topology as well as to simulate the learning, validation and testing phases without imposing any functional relationships between independent and dependent variables. With this architecture, ANN methodology has proven to be a powerful Black box model, which excels at function approximation and pattern recognition. Added to that, it is more robust and flexible than other types of black box models. Several artificial neural networks are applied in order to obtain the best structure for the study area. Two popular neural network models are the Feedforward Neural Network (FNN) and Recurrent Neural Network (RNN). For training these networks different algorithms can be used. In the present research, gradient descent with momentum and adaptive learning rate backpropagation (GDX), Levenberg–Marquardt (LM), and Bayesian Regularization (BR) are used. Some studies provide details of the used networks and algorithms in ANN modeling (e.g. Coulibaly *et al.*, 2001a; Nadiri *et al.*, 2006).

Network Architecture

Several aspects of the architecture of neural networks that focus on the prediction of variables associated with hydrology are covered by Maier and Dandy (2000). Their suggestions were followed in the development of the current model. The structure of the network is determined by trial and error. The size of the input and hidden layer of the network has been variable, depending on the prediction horizon, whereas the output layer has a single node. The number of nodes in the hidden layer and the stopping criteria were optimized in terms of obtaining precise and accurate output. Finally, the activation function of the hidden layer was set to a hyperbolic tangent sigmoid function as this proved by trial and error to be the best in depicting the non-linearity of the modeled natural system, among a set of other options (linear and log sigmoid). It is noteworthy that there is no well established direct method for selecting the number of hidden nodes for an ANN model for a given problem. Thus the common trial-and-error approach remains the most widely used method.

Criteria of Evaluation

Two different criteria are used in order to evaluate the effectiveness of each network and its ability to make precise predictions. The Root Mean Square Error (RMSE) calculated by,

$$RMSE = \sqrt{\frac{\sum_{i=1}^{N}(y_i - \hat{y}_i)^2}{N}} \quad \ldots (1)$$

where y_i, $\hat{y}_i$, and N are the observed data, the calculated data and the number of observations, respectively. RMSE indicates the discrepancy between observed and calculated values. The lower the $RMSE$, the more accurate the prediction is. Also, the R^2 efficiency criterion (determination coefficient), is given by,

$$R^2 = 1 - \frac{\sum(y_i - \hat{y}_i)^2}{\sum(y_i - \bar{y}_i)^2} \quad \ldots (2)$$

which represents the percentage of the initial uncertainty explained by the model. The best fit between observed and calculated values, which is unlikely to occur, would have $RMSE = 0$ and $R^2 = 1$.

STUDY AREA AND DATA

The study area is located in the Tabriz plain (Figure 1), northwestern Iran. The Tabriz area lies in east Azarbaijan province, which is structurally part of the central Iran unit. It is wedged between the Zagros and Alborz mountain systems. The area includes formations of Devonian to Quaternary age affected by various geologic movements, most strongly those of Alpine origin. The mean elevation is 1340 m above sea level. The prevailing climate of the Tabriz area has semi-arid characteristics. During the wet season, the

area is under the influence of middle-latitude westerlies, and most of the rain that occurs over the region during this period is caused by depressions moving over the area, after forming in the Mediterranean Sea on a branch of the polar jet stream in the upper troposphere. The average annual rainfall is 261.1 mm, during 1950 until 2005 years. The mean daily temperatures vary from –22°C in January up to 40°C in July with a yearly average of 9°C. The dominant winds over the area blow from the northeast and the southwest. In general, mean monthly relative humidity at the Tabriz Airport meteorological station is relatively high during the November–February period, ranging from 75 to 80%, and lower during July and August, when it is about 35 to 45%. Pan evaporation measured during the water year 2005–2006 was 1294 mm, (the water year has been fixed from the 20th September to 19th September of the following year and is used in all hydrologic discussions). The Ajichay River is the only perennial river in the study area and other temporal drainages join this main river. The Tabriz area formations are composed of Miocene faces that have covered alluvial sediments unevenness and have formed steep strata east to west. Miocene bedrock in this area is high, so alluvial sediment is very thin. Tabriz city in the southeast and south overlies Miocene beds and Plio-Quaternary faces that consist of semi compressed conglomerate beds with sandstone, carbonate, tuff, agglomerate and marl. These formations have formed the Tabriz aquifer.

A quantitative study of the piezometric fluctuations accounts for the general tendencies of seasonal or interannual variations that are translated in a very different way according to the hydrogeologic context. Annual piezometric fluctuations depend on the aquifer hydraulic characteristics, the position of the basin upstream and downstream limits, the groundwater depth, the replenishment time, and essentially the internal aquifer geometry. These characteristics are the major parameters intervening in the mode and the chronology of the piezometric events. By analyzing the piezometric map (lower water bodies) (Figure 2), we can distinguish, despite the existence of some anomalies in direction of groundwater flow, the general direction of groundwater in study area which is east to west. The cause of these anomalies is over-abstraction of pumping wells in farming field (central and southwest of map). The data utilized in this study were collected over 10 years (from April 1995 to March 2004) with a 1 month time interval. The data collected consist of the following categories: (i) observed piezometry of 16 piezometers (Central (CP), 2, 3, 4, 5, 6, 7, 8, 9, 10, 11, 12, 13, 14, 15, 16), (ii) rainfall in Tabriz airport station, (iii) mean temperature in Tabriz airport station, (iv) discharge of Ajichay river in Vaniyar station. Figure 2 shows positions of piezometers in the study area.

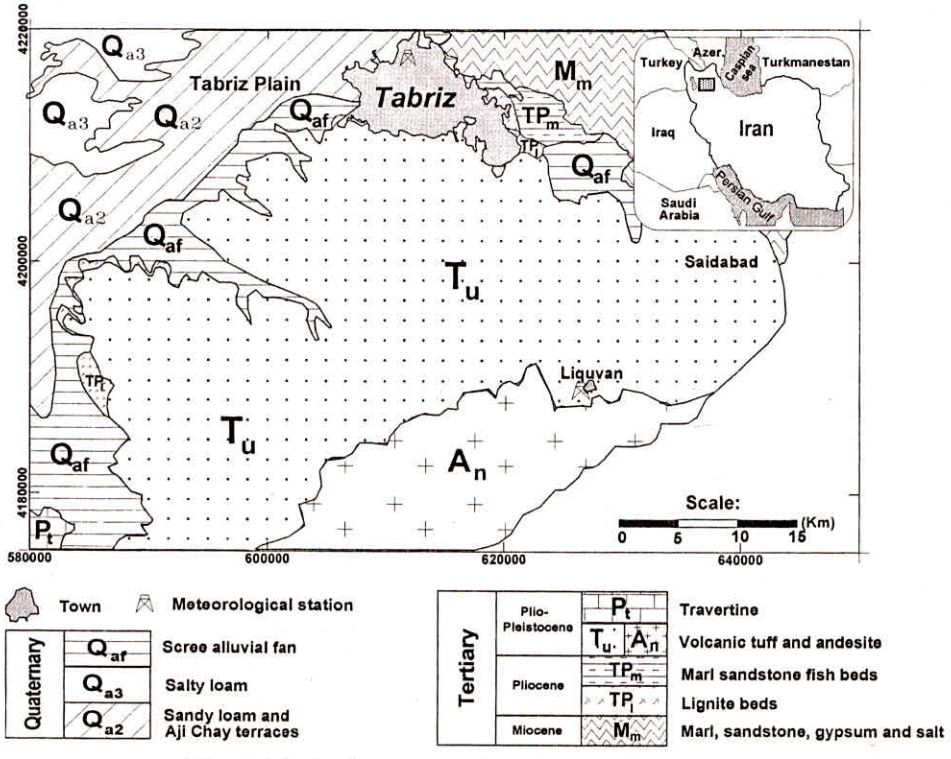

Fig. 1: Geologic map and localization of study zone

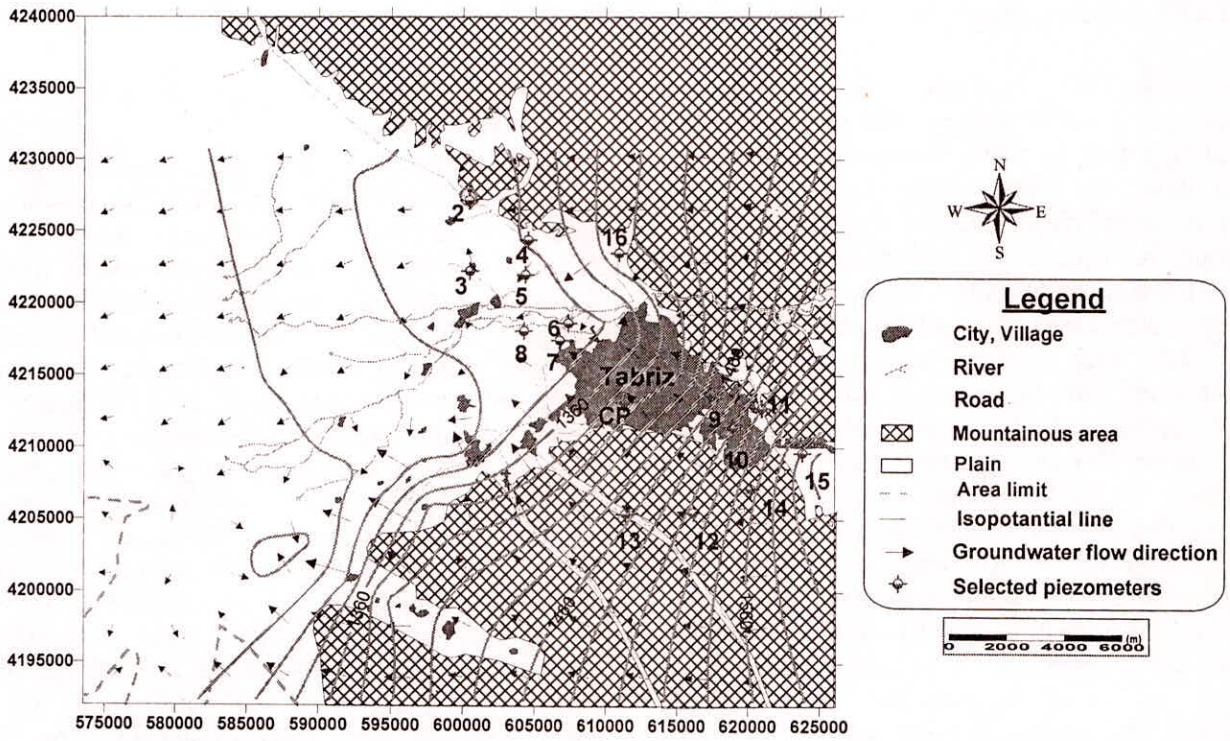

Fig. 2: Groundwater flow direction, piezometric map and positions of piezometers

RESULTS AND DISCUSSION

After the number of neurons in the first, hidden and last layers were fixed. In order to make the results statistically more plausible, three different partitions of the normalized database were used for simulation. The database was divided into training, validation and test groups. For the ANN models described in this paper, 60% of the available data were used for training, 20% were used for the validation and 20% were reserved for testing. There are two important steps in ANN modeling. The first is to ensure that the network extracts the necessary features from the data. This is based on processing training data of the ANN, which must be available for learning purposes. The training data base must be sufficiently representative to provide adequate knowledge retrieval, as needed in future reasoning activities of the Neural Network (NN). The percentage of data needed for training, validation and testing are problem specific. However, in this study, several models were tried with percentages of training data varying from 45 to 60%. The second important step in ANN modeling is to find the optimal number of neurons in the hidden layer which was discussed before.

According to recent researches (Coulibaly *et al.*, 2001a; Lallahem *et al.*, 2005), effective factors in the fluctuation of groundwater are temperature, rainfall, and mean discharge of basin. Because of typical hydrology and hydrogeology of every basin, effective delay times of each factor for special basins are different. In this study, for finding the best ANN model structure for the study area, a piezometer that has overall characteristics of the study sector was used. This piezometer called Central Piezometer (CP) (Figure 2). Therefore, to reach the best data set and delay time (t_o is present time and 1 month lag toward forecasting time), the following data set as input neurons are examined: (i) temperature, rainfall and discharge of Ajichay River (with t_o and t_o–1delay), water level in CP piezometer (with t_o, t_o–1 and t_o–2 delay) and water level in two nearest lateral piezometer (with t_o and t_o–1 delay), (ii) temperature, rainfall and discharge of Ajichay River (with t_o and t_o–1 delay), water level in CP piezometer (with t_o, t_o–1 and t_o–2 delay), (iii) temperature, rainfall and discharge of Ajichay River (with t_o and t_o–1 delay), water level in CP piezometer (with t_o and t_o –1 delay), (iv) temperature, rainfall and discharge of Ajichay River (with t_o delay), water level in CP piezometer (with t_o delay). Each of data set is used to train by (13, 7, 1) (i.e., 13 nodes in input, 7 nodes in hidden, 1 node in output layers), (9, 6, 1), (8, 5, 1), (4, 2, 1) structures respectively. Table 1 shows the results of considering structures with different input data sets. The target vector of structures for whole data set was water level forecasting during 24 months (2003–2004).

Table 1: RMSE% of 6 Networks-Algorithms with Different Input Data

Data Set	*FNN-BR*	*FNN-GDX*	*FNN-LM*	*RNN-LM*	*RNN-BR*	*RNN-GDX*
4	8.83	5.48	4.13	5.8	9.25	6.05
3	9.18	6.23	4.76	5.93	10.08	6.53
2	9.54	6.9	5.24	6.41	10.45	7.4
1	10.13	7.25	5.9	7.35	10.43	7.95

The results, presented in Table 1, revealed that the best data set is 4. Therefore, groundwater fluctuation effective parameters in the study sector for ANN models are just temperature, rainfall and discharge of Ajichay River (with t_o delay), and water level in CP piezometer (with t_o delay). Fluctuations of water level in the nearest lateral piezometers have intangible effects on the central piezometer water level. Its reason can be the complexity of Tabriz aquifer. To reach a high efficiency structure for study area, the fourth data set is used.

For every input variables (fourth data set), the time series was divided into 3 different subsets: One subset for training the neural network (1995–2000), one for model validation (2001–2002) and one for model testing (2003–2004). Since our goal is to predict future groundwater depths, any information concerning aquifer fluctuation was considered as it would inhibit the efficiency of our data driven model. All tests and results were derived through programming in Matlab 7.1. By means of trial and error, an optimum network and parameter configuration for all two networks (FNN, RNN) were derived. The input layer in all networks consisted of 4 input nodes for precipitation, temperature, and stream flow and groundwater level. The output of the network is a prediction of the well level at time step $t_o + 1$. The number of hidden neurons for both RNN and FNN was determined to 2 through trial and error. Consideration of the data set was based on the results of Table 1, in the calibration step. This number of neurons seems to be both time efficient and adequate to handle the rather small amount of data of the problem considered. Other parameters that were adjusted in order to achieve more accurate results were the goal value of the error function of the network during calibration, calculated by the Root Mean Square Error (RMSE) and determination coefficient (R^2), the learning rate of the training algorithms, the number of epochs or feeds of each network. The need for adjustment of these parameters lies in the danger of overtraining a network, an effect that is analogous to over-fitting a polynomial function. The best overall performance for the given problem was achieved by the feedforward network trained with the Levenberg–Marquardt algorithm and the second best by the recurrent neural network trained with the same algorithm. As we can see from Table 3, even though the feedforward network trained with the GDX algorithm seems to explain the groundwater level change ($R^2 = 0.785$), its results are shifted, rendering the method unsuitable for the problem.

The most unsuitable network was the recurrent neural network trained by the Bayesian regularization algorithm. This may indicate that RNN requires more complex training algorithms (Coulibaly *et al.*, 2001a, b, c). The rest of the networks performed relatively well but tended to overestimate the observed dataset.

Table 2: R^2 and RMSE for Training Step

Criterion	*Network*					
	FNN-BR	*FNN-GDX*	*FNN-LM*	*RNN-LM*	*RNN-BR*	*RNN-GDX*
R^2	0.692	0.901	0.985	0.911	0.672	0.83
RMSE%	8.52	5.18	2.11	3.42	8.81	5.69

Table 3: R^2 and RMSE for Testing Step

Criterion	*Network*					
	FNN-BR	*FNN-GDX*	*FNN-LM*	*RNN-LM*	*RNN-BR*	*RNN-GDX*
R^2	0.592	0.785	0.865	0.818	0.554	0.668
RMSE%	9.72	6.84	3.61	4.52	9.92	7.73

Also all the networks performed well for 1 month ahead predictions. The most promising techniques seem to be those using the feedforward neural network trained with the Levenberg–Marquardt algorithm that underestimates part of the groundwater level during 24 months (2003–2004). The physical meaning of this result is that the structure of this model allows its weights to adjust values that depict the trends of the natural system we are simulating. For validatoig purposes, a 24 month-ahead prediction is made and compared with observed values. Figure 3A and B show how 6 combinations predicted groundwater levels for this 24 month period (2003–2004). After achieving the best structure and data set for forecasting the study area groundwater level, in order to present the spatiotemporal pattern, modeling of other piezometers than the central piezometer model is necessary. Because presentation of spatiotemporal model by ANNs for groundwater level is an innovation that has not been carried out, it had a great deal of difficulty because of the limitations of ANN applications for spatial forecasting. The first step is to prepare models for selected piezometers (2, 3, 6, 10, 16, 8, and 13) among the study area piezometers (2, 3, 4, 5, 6, 7, 8, 9, 10, 11, 12, 13, 14, 15, and 16) and the rest of the piezometers are employed to test the model. In order to prepare each model of selected piezometers all steps that are carried out for the presentation of the central piezometer model previously are performed. Because the weights and biases of each selected piezometers model are required, the inputs and output neurons are fixed, the most important point in modeling the considered piezometers is fixing hidden layer neurons. Table 4 shows summarized results of the training, validation and testing steps for selected piezometers networks with (4, 2, 1) structure.

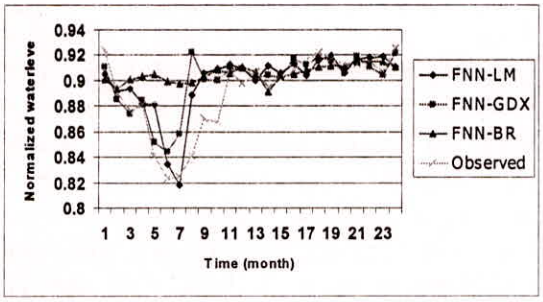

(A)

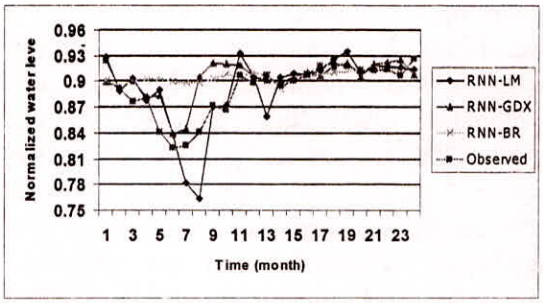

(B)

Fig. 3: Comparison of testing results with observed values. (A) FNN networks (B) RNN networks

Table 4: Results of Selected Piezometers in the Training, Validation and Testing Steps

Piezometer			2	3	6	10	16	8	13
Criterion	Training Step	RSME%	5.4	6.5	6.6	5.3	4.9	5.3	4.1
		R^2	0.93	0.91	0.94	0.98	0.93	0.97	0.98
	Validation Step	RSME%	4.9	7.7	7.2	6.5	5.7	5.8	4.9
		R^2	0.87	0.88	0.86	0.96	0.88	0.93	0.95
	Test Step	RSME%	7.5	8.4	7.7	8.6	6.1	6.3	5.4
		R^2	0.85	0.79	0.81	0.93	0.81	0.88	0.9

According Table 4 and considering the assumed limitation in fixing nodes in the input layer (4), output layer (1) and hidden layer (2), the obtained results of the considered piezometers models are acceptable.

The algorithm of the method for spatiotemporal forecasting is explained by the following steps:

1. Extraction of weights and biases from the ANN which was used for each piezometer modeling with fixed nodes in the layers.
2. Classification of node weights with the same position for whole models.
3. Consideration of correlation between position of piezometers and every class of weights and biases.
4. Framing spatiotemporal ANN model (4, 2, 1) with obtained weights and biases by regression relations.
5. Testing spatiotemporal model for different locations of the study area.

Table 5 presents the obtained weights and biases of the considered piezometer models. In Tables 5–9 w and b present the abbreviation of weights and biases, respectively; in this manner subscript numbers show the number of node and its order, respectively. After classification of the same order and the number of weights and biases, vectorial distance (R) of each piezometer from a fixed assumed point as the area origin (left corner of study area map, Figure 3, X = 590000 m, Y = 4200000 m) is obtained by,

$$R = \sqrt{X^2 + Y^2} \quad \ldots (3)$$

where X and Y are coordinates from the left corner of the study area map (X = 590000 m, Y = 4200000 m). Then correlation between similar vectorial distance of each piezometer and their classified weights and biases of the ANN models are computed by Table curve and Curve expert software. The most accurate fitted functions with the determination coefficient values accompanying relevant coefficients are shown in Tables 6, 7 and 8.

The next step is cross validation the presented spatiotemporal model that is carried out by the remaining piezometers. The weights and biases of the remaining piezometers are computed by the obtained regression functions (Table 6–8) and are shown in Table 9.

Table 5: (A) The Hidden Layer Weights (B) The Output Layer Weights and Biases of the Model

(A)

Piezo-meter	W_{11}	W_{12}	W_{13}	W_{14}	W_{15}	W_{16}	W_{17}	W_{18}	R (km)
2	–0.6287	–0.9939	0.50113	–2006.8	–0.291	–2.0624	44.4423	–322.88	28.3832697
3	0.00175	0.00318	–0.0046	–20.252	0.54547	1.4005	–0.2393	1.1401	24.5818022
6	0.01129	0.00636	–0.0221	–18.613	–0.5038	–0.5187	–12673	–2.7048	25.438406
10	–1.3856	–2.1649	4.6241	2.4252	0.00324	0.01273	–0.0145	22.2704	31.0671853
CP	2.7978	0.62244	–0.1739	2.2545	2.0217	0.44971	–0.0018	–1.542	33.9040558
16	0.01169	0.00267	0.00534	–15.197	–13.092	–8.8225	–7.287	2.0205	31.4327158
8	0.02051	0.02283	–0.0593	–45.269	0.22109	0.71749	0.05986	2.2187	23.0054341
13	–1.986	–0.0353	–0.4794	–2.128	0–0.41336	–0.0741	–0.0888	150.842	22.0223182

(B)

Piezometer	w_{21}	w_{22}	b_{11}	b_{12}	b_2	R (km)
2	–2.2445	10.3713	2006.69	325.24	–4.9294	28.3832697
3	–26.305	7.7776	20.6878	1.7057	7.3127	24.5818022
6	–11.314	–2.8082	18.8005	–3.0544	3.2273	25.438406
10	9.5687	25.4565	1.6502	–22.95	9.6817	31.0671853
CP	9.5687	25.4565	–4.7019	–1.1011	0.35805	33.9040558
16	–18.318	–0.0651	14.7337	3.465	–3.8429	31.4327158
8	–7.9254	1.3149	44.9302	2.6601	0.31107	23.0054341
13	–19.094	35.8551	–2.7821	–152.71	19.3729	22.0223182

Table 6: The Best Fitted Functions (y is the weight and x = R) for the Hidden Layer Weights

Weights	*Function*	*Parameters*	*Values*	R^2
W_{11}	y = a+bx+cxlnx+dx3+ex/lnx	a	1.16E+06	0.936475
		b	297162.6331	
		c	–30552.1915	
		d	0.450715084	
		e	–7.90E+05	
W_{12}	Y = a+bsin(2px/d+c) [Sine]	a	–1.89E+00	0.829956
		b	2.413556512	
		c	5.930573738	
		d	0.422417641	
W_{13}	y = a + bexp(–0.5((x–c)/d)2) [Gaussian]	a	–1.48E–01	0.992059
		b	736.0165883	
		c	29.83688414	
		d	0.387566341	
W_{14}	y–1 = a+blnx/x2+c/x2	a	1.93E+00	0.999286
		b	–2004.8193	
		c	5155.253455	
W_{15}	y–1 = a+b/lnx+clnx/x	a	–1.40E+04	0.837689
		b	81790.01484	
		c	–88495.8744	
W_{16}	Y = a + bsin2(2px/d+c) [Sine2]	a	–6.37E+00	0.745276
		b	8.062575404	
		c	3.268853494	
		d	0.515304734	
W_{17}	y–1 = a+bex+ce–x	a	3.07E–02	0.999995
		b	–3.60E–15	
		c	–3.39E+09	
W_{18}	y–1 = a+b/x2+ce–x	a	2.89E–01	0.991812
		b	–235.470934	
		c	7.45E+08	

Table 7: The Best Fitted Functions for the Output Layer Weights

Weights	*Function*	*Parameters*	*Values*	R^2
W_{21}	y = a+bx+cx2.5+dx3+eex	a	3.31E+03	0.642244
		b	–322.457533	
		c	3.87242503	
		d	–0.47125558	
		e	1.55E–13	
W_{22}	y = a+bx+cx3+dex+ee–x	a	–4.96E+02	0.697245
		b	26.0580591	
		c	–0.01013631	
		d	6.10E–14	
		e	2.38E+11	

Table 8: The Best Fitted Functions for Biases

Biases	*Function*	*Parameters*	*Values*	R^2
b_{11}	y = a+berfc(((x–c)/d)2) [Erfc Peak]	a	1.25E+01	0.99949
		b	2076.92445	
		c	28.04577402	
		d	1.795072563	
b_{12}	y = a+b/(1+((x–c)/d)2) [Lorentzian]	a	–2.71E+01	0.625664
		b	1975.043005	
		c	28.07174037	
		d	0.384661451	
b_{22}	y = a+bx+cxlnx+dx3+ex/lnx	a	–1.99E+07	0.666212
		b	–5.10E+06	
		c	524234.0068	
		d	–7.58207569	
			1.36E+07	

Table 9: (A) Weights of the First Layer Nodes, (B) Weights and Biases of the Second Layer Nodes and the First Layer Biases

(A)

Piezometer	W_{11}	W_{12}	W_{13}	W_{14}	W_{15}	W_{16}	W_{17}	W_{18}	*R (km)*
4	–0.6923	–0.0679	0.50113	–2007	–0.7871	–3.5457	46.6329	–322.88	28.3833
5	–0.2979	–0.998	–0.1479	–10.041	–0.9107	–5.2714	61.9132	–19.931	26.2391
7	0.23925	–0.2051	–0.1479	–5.556	0.51951	–3.2212	–12.636	–11.031	24.1535
9	–0.812	0.37248	124.555	9.43603	–2.375	–0.5724	–26.809	27.126	30.5672
12	–0.4027	–0.6234	–0.1479	–12.436	–0.7729	1.36554	48.864	–24.884	26.6732
15	–0.7379	–0.9627	5.57269	7.73302	–4.4578	1.6125	–12.699	22.4489	34.65

(B)

Piezometer	w_{21}	w_{22}	b_{11}	b_{12}	b_{22}	*R (km)*
4	–0.1943	12.5773	2006.59	325.24	–2.0235	28.3833
5	–10.135	6.09413	328.13	20.5795	4.59816	26.2391
7	–18.868	–1.2339	12.474	11.4011	1.88915	24.1535
9	–1.5701	12.6828	23.414	–28.116	–1.1424	30.5672
12	–7.7776	7.83762	860.548	25.6827	3.61238	26.6732
15	–4.0145	12.0435	12.638	–23.259	0.85197	34.65

These parameters are used for forecasting the water level in the left piezometers and then the computed results are compared with observed water levels. The results of the considered models are summarized in Table 10. In this way this model was qualified for forecasting water level in the whole of study sector even without any piezometers. According to the results, the efficiency of the model has an inverse relation with the piezometer distance of central piezometer. Therefore, in addition to incredible advantage of the presented model, it has also limitations. As can be seen in Table 10, the best result is related to piezometer 9 that is the nearest piezometer to the central piezometer. The results of other piezometers are also acceptable but it is clear the aquifer has high complexity. It causes to the efficiency of the same structures to have different values (0.65–0.82). So the most important factor in the model result can be the complexity of the aquifer and the position of every piezometer.

Table 10: Results of Left Piezometer Forecasting

Piezometer		4	5	7	9	12	15
Criterion	RMSE%	4.9	5.8	5.7	4.1	5.9	6.9
	R^2	0.81	0.79	0.69	0.82	0.65	0.68

CONCLUSION

Neural networks have proven to be an extremely useful method for empirical forecasting of hydrological variables. In this paper, an attempt was made to identify the most stable and efficient neural network configuration for predicting groundwater level in the Tabriz aquifer and to present a spatiotemporal model as an innovation. Tabriz aquifer is complex and multilayered so it is quite difficult for modeling and groundwater level forecasting. The total of six different ANN configurations were tested in terms of optimum results for a prediction horizon of 24 months. The most suitable configuration for this task was proved to be a 4–2–1 feedforward network trained with the Levenberg-Marquardt method as it showed the most accurate predictions of the decreasing groundwater levels. Then optimal structure is applied for forecasting of selected water level piezometers in Tabriz aquifer. From the results of the study it can be inferred that the Levenberg-Marquardt algorithm is more appropriate for this problem, since RNN also performs well when trained with this method. This structure is also used for presenting the spatiotemporal model. According to presented algorithms this model is obtained by computing the correlation of vertical distance of the assumed point with weights and biases of models. In this way all of the piezometer water levels in the study area can be forecasted by using the obtained weights and biases based on regression functions. In general, the results of the case study are satisfactory and demonstrate that neural networks can be a useful spatiotemporal prediction tool in the area of groundwater hydrology. Most importantly, this paper presents indications that neural networks can also be applied in cases where the aquifer is complex and we need, in addition to temporal ,prediction, spatial forecasting. In this research, it was tried to use the vectorial distance as a spatial factor (R) but in opinion of the authors, it will be better to use local coordinate of every considered piezometer (i.e., X, Y), in stead of vertical distance (R). This suggestion can be studied another research topic.

REFERENCES

ASCE Task Committee on Application of Artificial Neu Networks in Hydrology, 2000. Artificial neural netwo in hydrology, parts I and II. J. Hydrol. Eng., 5(2), 115–13

Beaudeau, P., Leboulanger, T., Lacroix, M., Hanneton, and Wang, H.Q. (2001). Forecasting of turbid floods i karstic drain using an artificial neural network. Grou Water, 39(1), 139–160.

Coulibaly, P., Anctil, F., Aravena, R. and Bobe´e, (2001a). Artificial neural network modeling of water ta depth fluctuations. Water Resour., Res. 37(4), 885–89

Coulibaly, P., Anctil, F. and Bobe´e, B. (200 Multivariate reservoir inflow forecasting using tempo neural networks. J. of Hydrol. Eng., 9–10, 367–376.

Coulibaly, P., Bobee, B. and Anctil, F. (2001c). Improv extreme hydrologic events forecasting using a r criterion for artificial neural network selection. Hyd Process., 15, 1533–1536.

French, M.N., Krajewski, W.F. and Cuykendall, R (1992). Rainfall forecasting in space and time usin neural network. J. of Hydrol., 137, 1–31.

Govindaraju, R.S. and Ramachandra Rao, A. (20 Artificial Neural Networks in Hydrology. Klu Academic Publishing, The Netherlands.

Hagan, M.T., Demuth, H.B. and Beale, M. (1996). Ne Network Design. PWS, Boston

Kohonen, T. (1988). An introduction to neural comput Neural Networks, 1(1), 3–16.

Kurup, U.P. and Dudani, N.K. (2002). Neural networks profiling stress history of clays from PCPT data Geotech. Geoenviron. Eng., 128(7), 569–579.

Lallahem, S. and Mania, J. (2002). A linear and non-li rainfall–runoff models to evaluate aquifer outfl Tribune de l'Eau., 55(4), 615.

Lallahem, S. and Mania, J. (2003a). Evaluation forecasting of daily groundwater inflow in a small cha watershed. Hydrol. Processes, 17, 1557–1561.

Lallahem, S. and Mania, J. (2003b). A non-linear rain runoff model using neural network technique: exampl fractured porous media. J. Math. Comput. Model., 1047–1061.

Lallahem, S., Mania, J., Hani, A. and Najjar, Y. (2005). the use of neural networks to evaluate ground w levels in fractured media. J. of Hydrol., 307, 92–111.

Luck Kin, C., Ball, J.E. and Sharma, A. (2001). application of artificial neural networks for rai forecasting. Math. Comput. Model., 33, 683–693.

Maier, H.R. and Dandy, G.C. (2000). Neural network for the prediction and forecasting water resources variables: a review of modeling issues and applications. Environ. Modeling Software, 15, 101–124.

Nadiri, A.O., Mogaddam, A.A. and Nourani, V. (2006). Basics of artificial neural networks model (ANNs) and its application in hydrogeology. Proceeding of the 24th Symposium of Geosciences, Geological Survey of Iran, Tehran, Iran.

Parkin, G., Younger, P.L., Birkinshaw, S.J., Murray, M. and Rao, Z. (2001). A new approach to modelling river–aquifer interactions using a 3-D numerical model and neural networks, Impact of Human Activity on Groundwater Dynamics, Proceedings of a Symposium held during the Sixth IAHS Scientific Assembly at Maastricht, The Netherlands, IAHS Publ., No. 269.